Experimental Investigation of Steel Lap Welded Pipe Joint Performance under Severe Axial Loading Conditions in Seismic or Geohazard Areas

Brent D. Keil[1]; Gregory Lucier[2]; Spyros A. Karamanos[3]; Richard D. Mielke[4]; Fritz Gobler[5]; Dimitris Fappas[6]; Gregory C. Sarvanis[7]; Giannoula Chatzopoulou[8]; and Robert J. Card[9]

[1]Northwest Pipe Co., Vancouver, WA. Email: BKEIL@nwpipe.com
[2]North Carolina State Univ., Raleigh, NC. Email: gwlucier@ncsu.edu
[3]Univ. of Thessaly, Volos, Greece. Email: skara@mie.uth.gr
[4]Northwest Pipe Co., Vancouver, WA. Email: RMIELKE@nwpipe.com
[5]Northwest Pipe Co., Vancouver, WA. Email: fgobler@nwpipe.com
[6]Univ. of Thessaly, Volos, Greece. Email: dimitrisfp@gmail.com
[7]Univ. of Thessaly, Volos, Greece. Email: gsarvan@uth.gr
[8]Univ. of Thessaly, Volos, Greece. Email: gihatzop@uth.gr
[9]Lockwood, Andrews & Newnam, Inc., Houston, TX. Email: RJCard@lan-inc.com

ABSTRACT

Welded lap joints are commonly used in large-diameter steel pipelines for water transmission. Their structural performance constitutes a key consideration for safeguarding pipeline integrity with no loss of pressure containment, required after a severe seismic, or geohazard event. Full-scale experiments are presented, which are part of an extensive ongoing project related to structural performance of welded lap joints under severe ground-induced (seismic) actions. The paper describes a series of large-scale physical experiments on 24-in. diameter steel pipes with welded lap joints subjected to axial compression and tension. The axial loading experiments under consideration complement the series of large-scale bending tests performed in 2017, and presented in the ASCE 2018 Pipelines Conference (paper entitled: "Experimental Results of Steel Lap Welded Joints in Seismic Conditions", authored by Keil et al.). The specimens tested under axial loading are first pressurized to 40% of yield pressure, and subsequently subjected to large amount of compression or tension. Measurements of the axial load, characteristic displacements, and local strains at the joint area have been obtained. All specimens exhibited the capability of sustaining high axial loads with significant axial deformation, without loss of pressure containment. In support of the above experiments, advanced finite element models have also been developed, for the purpose of simulating the experiments and elucidating some pertinent topics on the structural response of welded lap joint behavior. The results of the present study demonstrate the remarkable strength and deformation capacity of lap welded joints under consideration, supporting the argument that those joints can be used in steel pipelines crossing seismic and geohazard areas, where severe and permanent ground-induced actions are expected.

INTRODUCTION

Welded steel pipelines, used for water transmission, are often constructed in geohazard (seismic) areas, which may experience severe permanent ground deformation induced by fault rupture, liquefaction, soil subsidence, or slope instability. Those actions may threaten the structural integrity of the pipeline. The seismic design framework of water pipelines has been

described recently by Karamanos *et al*. (2017a). Within that framework, the deformation capacity and strength of lap welded joints has been identified as a consideration for further investigation.

Welded lap joints are often employed in large-diameter steel water transmission pipelines, and consist of a cold-formed "bell" at the end of each pipe segment, where the end of the adjacent pipe segment, often referred to as "spigot", is inserted and welded to the bell through a single or double full-circumferential fillet weld, as shown in **Figure 1**. The structural performance of welded lap joints against axial loading has been investigated by several researchers. An extensive literature review on this topic is presented in Karamanos *et al*. (2015) and (2017b). Nevertheless, the majority of these previous works focused mainly on non-seismic conditions, associated with relatively low axial compression or tension. Recently, the bending response of lap welded joints has been analysed in detail by the authors; experimental results have been presented by Keil *et al*. (2018), whereas numerical simulations have been presented by Chatzopoulou *et al*. (2018) and Sarvanis *et al*. (2019), in an attempt to determine their strength and the deformation capacity under extreme bending conditions.

The above recent works of the authors are part of a large-scale research program, sponsored by Northwest Pipe Company, aiming at safeguarding the structural integrity of welded lap joints of steel water pipelines constructed in geohazard (seismic) areas. The present paper is also part of this research program, extending and supplementing the bending experiments presented by Keil *et al*. (2018), with a series of axial loading tests. More specifically, the paper describes a series of nine large-scale experiments on welded lap joints in 24-inch-nominal-diameter steel pipes. The specimens have been end-capped, pressurized to 40% of yield pressure, and subjected to either axial compressive or tensile loading. In each group of specimens, the lap welds have been "internal", "external" and "double", so that all possible weld types are examined. Measurements have been obtained for the applied axial load, characteristic displacements, and local strains at specific locations near the lap welded joint.

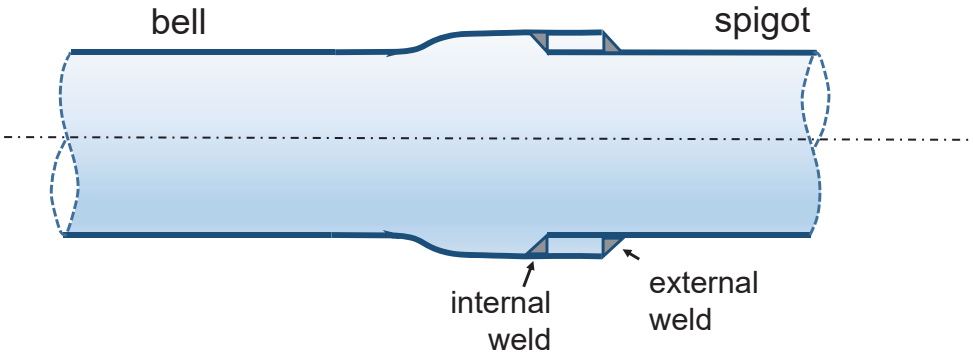

Figure 1. Schematic configuration of the lap welded steel pipe joint.

EXPERIMENTAL SETUP AND PROCEDURE

A total of nine (9) experiments were performed with all possible weld patterns of lap joints (double, single-internal and single-external): five (5) specimens have been tested under axial

tension, and four (4) specimens were subjected to axial compression. Details on the test specimens are tabulated in **Table 1** below.

The tests were performed in the facilities of Northwest Pipe Co., at Adelanto plant, California, and utilized pipes with outer diameter 25.75 in (654 mm) [nominal diameter NPS=24], and two thickness values equal to 0.135 in (3.429 mm) with material ASTM A1011 GR36 and 0.250 in (6.35 mm) with material ASTM A1018 GR42. The experimental setup for the axial tests, shown in **Figure 2**a, consists of two very stiff horizontal plates connected with four (4) vertical actuators with total capacity exceeding 1,573 kips (7,000 kN). The pipe specimens used in axial compression tests are 57 in (1,447 mm) long, while the specimens subjected to axial tension tests have a length of 48 in (1,219 mm).

All axial loading tests were performed in the presence of internal pressure, applied with the use of a hydraulic pump. Internal pressure was applied first at a level of 40% yield pressure ($p_Y = 2\sigma_Y t/D$), and subsequently, keeping the pressure level constant, axial loading was applied by controlling the vertical displacement of the hydraulic actuators. The load applied by the actuators, was recorded, together with joint shortening or elongation. The latter was measured using wire transducers that recorded the relative displacement of two points located on either side of the lap joint at 14 in from the end of the bell, corresponding to a total gage length L_0 equal to 28 in (711.2 mm), as shown in **Figure 2**b. More specifically, wire transducers were placed along three equally-spaced generators around the pipe cross-section, and the measured relative displacement ΔL was normalized by the corresponding gage length L_0, so that the ratio $\Delta L/L_0$ is obtained, which can be regarded as a "macroscopic" strain of the deformed joint.

In addition to load and displacements, local strains at the area of the lap joints were recorded at both the bell and the spigot side of the pipe specimen using strain gauges, placed in three equally spaced generators around the circumference of the specimens.

Figure 2. (a) Experimental setup for axial experiments; (b) wire transducers for the measurement of the normalized deformation of the joint $\Delta L/L_0$ (shortening or elongation).

RESULTS OF COMPRESSION EXPERIMENTS

Representative experimental results are presented in **Figure 3**, in terms of normalized force-displacement diagrams for axially-compressed specimens AC4-BD, AC3-ASI and AC1 - AD. In

these diagrams, the applied load was normalized using the yield (plastic) force of the pipe cross-section $F_Y = \sigma_Y A$, where A is the cross sectional area of the pipe cross-section, and σ_Y is the yield stress of the pipe material, equal to 43,900 psi (302 MPa) and 47,000 psi (324 MPa) for the thin and thick specimens, respectively. For the case of the thin-walled pipes (0.135-inch-thick), the plastic force F_Y is equal to 476 kips (2,121 kN), while for the thick-walled pipes (0.250-inch-thick) the plastic force F_Y is equal to 941 kips (4,186 kN). In all compressive experiments, the maximum load, referred to as "buckling load" of the lap welded joint, occurred at a displacement smaller than 0.28 in (7 mm), which corresponds to a normalized displacement $\Delta L/L_0$ equal to 0.98%. Beyond that stage, the post-buckling behavior of the specimen is characterized by a decrease of load, as shown in the three diagrams of **Figure 3**. The most remarkable result though is that the specimens were able to undergo substantial deformation, corresponding to $\Delta L/L_0$ values exceeding 12%, without exhibiting any loss of containment associated with fracture at the pipe wall near the weld(s).

An important observation; refers to the location of the buckle at the joint area, shown in **Figure 4** for the four specimens under consideration. More specifically, one specimen (AC3-ASI) buckled at the bell, one specimen (AC2-ASO) buckled at the spigot, whereas in two specimens (AC1-AD and AC4-BD) local buckles appeared simultaneously at the bell and the spigot. This indicates that the location of buckles may not be predicted and depends significantly on the presence of initial geometric or material imperfections in this area, mainly due to the bell manufacturing process.

Table 1. Details of test specimens.

loading	specimen	weld details	thickness (in)	D/t	pressure level (psi)
Axial compression	AC1-AD	double weld	0.250	103	325
	AC2-ASO	single (outside) weld			
	AC3-ASI	single (inside) weld			
	AC4- BD	double weld	0.135	191	170
Axial tension	AT1- AD	double weld	0.250	103	325
	AT2-ASO	single (outside) weld			
	AT3-ASI	single (inside) weld			
	AT4- BD	double weld	0.135	191	170
	AT5-BSI	single (inside) weld			

In **Figure 5**, representative tensile and compressive strains are presented in terms of applied displacement for tests AC1-AD. The experimental results indicate that the joints under consideration are capable of sustaining significant amount of local strain. In those axial compression tests, tensile and compressive local strains were measured exceeding 5%, without loss of pressure containment, a result which is compatible with the high values of macroscopic strain $\Delta L/L_0$ discussed above. The results from the compression experiments are summarized in **Table 2**. All compression tests have demonstrated that the lap welded joints under consideration performed very satisfactorily, sustained remarkable axial compressive deformation, and obtained a multi-folded final configuration without any fracture of the pipe material or weld.

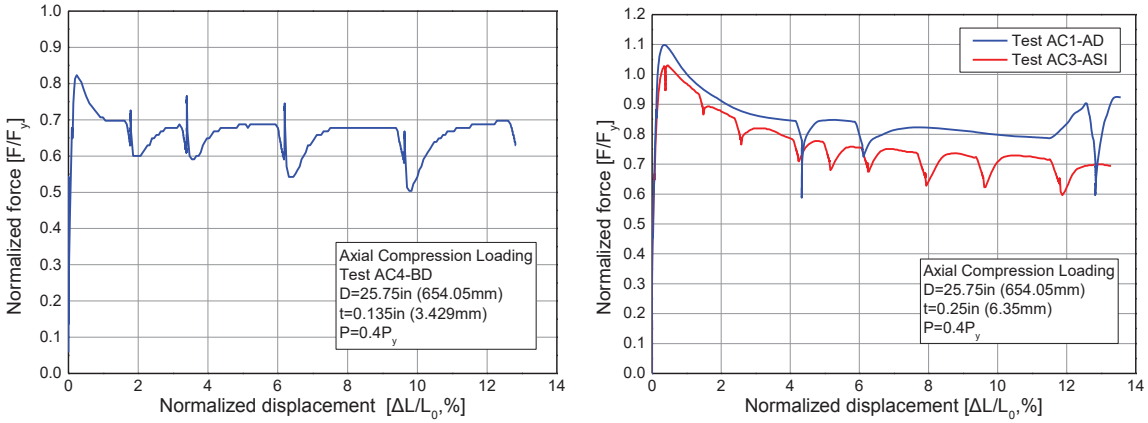

Figure 3. Normalized load-displacement curves under axial compression for three specimens: (a) thin-walled specimen AC4-BD (double welded); (b) thick-walled specimens AC1-AD (double welded) and AC1-ASI (single ID welded).

Figure 4. Local buckle patterns for axially-compressed specimens; (a) AC1-AD, (b) AC2-ASO, (c) AC3-ASI, (d) AC4- BD.

RESULTS OF TENSION EXPERIMENTS

The experimental results are presented in terms of normalized force-displacement diagrams **Figure 6** for specimens AT1-AD and AT2-ASO, whereas in **Figure 7** four fractured specimens are presented. In **Figure 6** the applied load has been normalized with the yield (plastic) force of

the pipe cross-section, which is equal to 941 kips (4,186 kN). The specimen with the double weld (AT1-AD) fractured at a normalized displacement $\Delta L/L_0$ equal to 19.8% and a maximum load equal to 1,429 kips (6,357 kN), while the specimen with the single outside weld (AT2-ASO) was fractured at a normalized displacement $\Delta L/L_0$ equal to 4.45% and a maximum load equal to 1,320 kips (5,875 kN). Both specimens exhibited significant strength (well above the plastic load of the pipe cross-section) and remarkable deformation capacity, especially the double welded specimen.

Table 2. Summary of results from compression experiments.

Specimen	D/t	maximum load (kips)	displacement at buckling (in)	maximum applied displacement (in)	location of buckle
AC1-AD	103	1,034	0.09	14.45	bell and spigot
AC2-ASO	103	1,071	0.26	10.08	spigot
AC3-ASI	103	967	0.09	12.87	bell
AC4- BD	191	392.5	0.06	7.76	bell and spigot

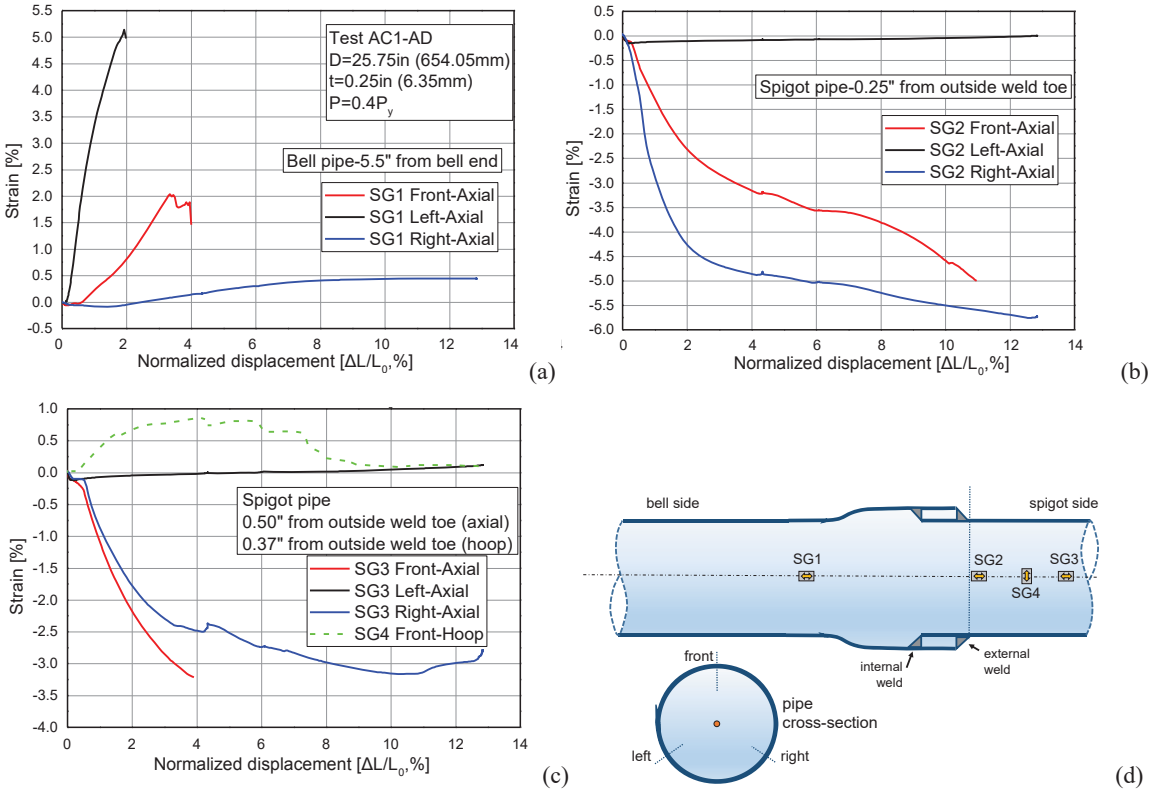

Figure 5. Strains plotted in terms of normalized shortening $\Delta L/L_0$ for specimen AC1-AD.

A summary of experimental results for tensile tests is offered at **Table 3**. It is important to notice that the specimens with double welds were capable to sustain a normalized displacement $\Delta L/L_0$ equal to 19.8% (thick-walled specimen) and 17.1% (thin-walled specimen), while the single welded specimens (inside or outside), were capable of sustaining a normalized displacement $\Delta L/L_0$ equal to 5.2% (thin-walled) and 4.4% (thick-walled).

Table 3. Summary of results from tension experiments.

Test	D/t	maximum load (kips)	displacement at fracture (in)
AT1- AD	103	1,429	5.55
AT2-ASO	103	1,320	1.25
AT3-ASI	103	1,653	1.24
AT4- BD	191	1,002	4.79
AT5-BSI	191	806	1.46

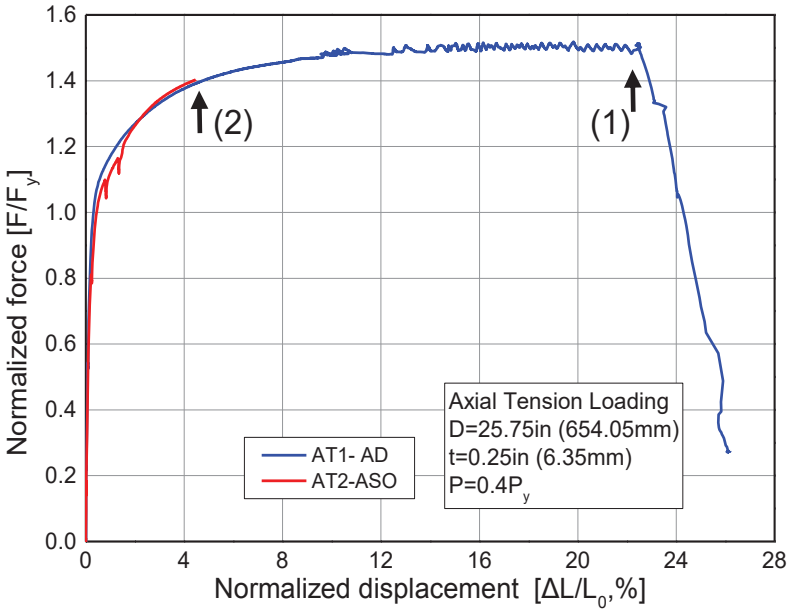

Figure 6. Normalized load-displacement diagrams under axial tensile load for thick-walled specimens AT1-AD (double welded) and AT2-ASO (single outside weld); the arrows (↑) on the diagrams indicate the stage at which failure due to fracture occurred: (1) for AT1-AD and (2) for AT2-ASO.

In **Figure 8** , local strains are presented in terms of applied displacement for specimen AT1-AD. Tensile and compressive strains measured at different locations in the vicinity of the joint are plotted against the applied normalized displacement. The experimental results indicate that the joint is capable of sustaining a significant amount of local strain, which exceeded 8% at the fracture stage. All tests have demonstrated that the welded lap joints under consideration have been capable of sustaining remarkable axial tensile strength and deformation, before fracture.

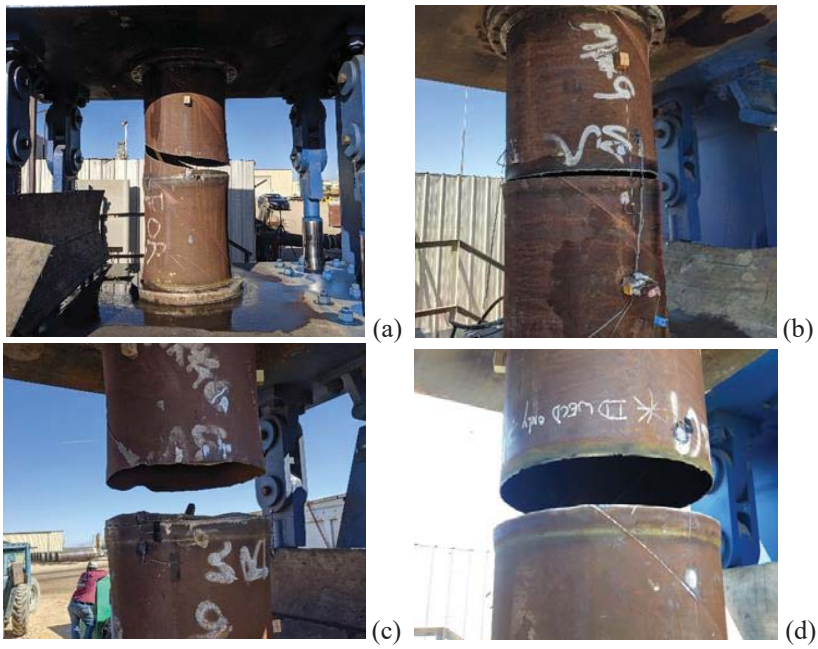

Figure 7. Fractured specimens under tensile loading; (a) AT1-AD, (b) AT3-ASI, (c) AT4-BD, (d) AT5-BSI.

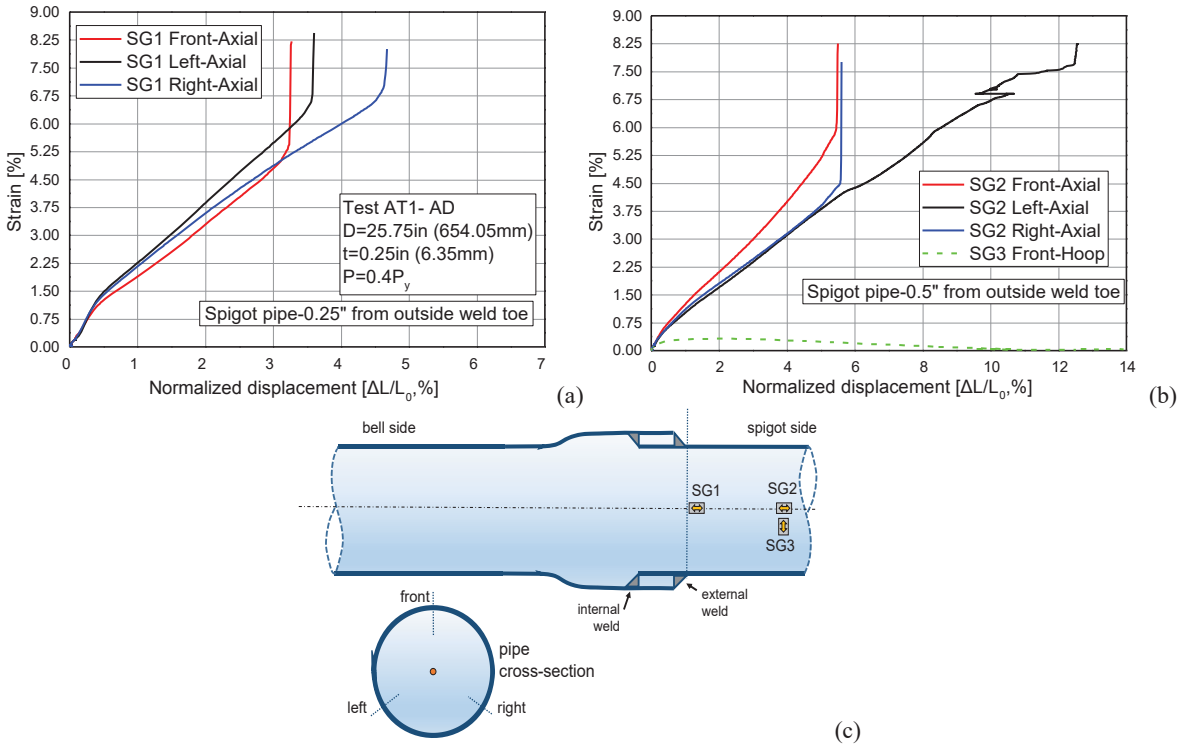

Figure 8. Measured strains platted with respect to the normalized elongation ($\Delta L/L_0$) of the joint for tension specimen AT1-AD.

NUMERICAL MODEL

The finite element model, developed by Chatzopoulou *et al*. (2018), has been employed for preliminary simulation of the experiments. It is presented briefly herein for the sake of completeness. The model consists of four main parts, a pipe with a bell configuration, a straight pipe (spigot), the outside weld and the inside weld, as shown in **Figure 9**. The model employs four-node, reduced-integration shell finite elements for the pipes and eight-node solid elements for the fillet welds. The gap size between the bell and the spigot is constant around the pipe and is equal to 0.05 inch, which is according to the AWWA C200 allowable value. The reader is referred to Chatzopoulou *et al*. (2018) and Sarvanis *et al*. (2019) for more information related to this model.

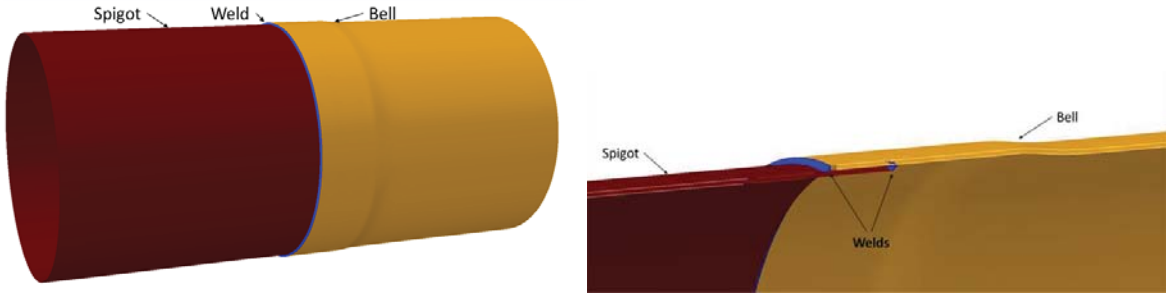

Figure 9. Finite element model of a welded lap joint; geometry of the double-welded area of the joint.

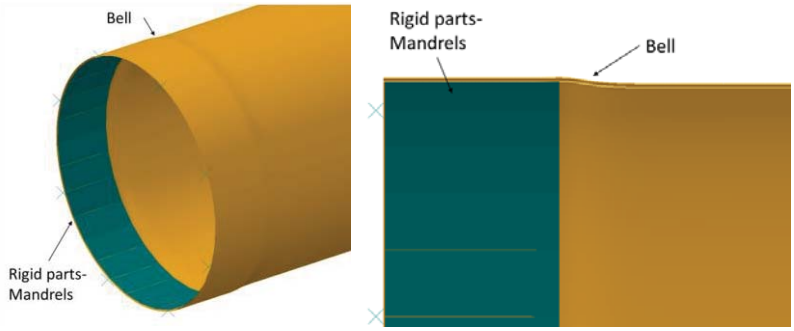

Figure 10. Numerical simulation of bell expansion.

Initially, bell expansion is simulated by expanding the pipe end, through an appropriate mandrel (modelled as rigid body) that moves outwards in the radial direction, as shown in **Figure 10**. In order to simulate the weld, the spigot and the bell are connected with the weld parts using appropriate kinematic constraints. Two reference points, located at each end of the model, are assumed, which are coupled in all six (6) degrees of freedom with the degrees of freedom of the end nodes of the pipe, in order to apply the boundary condition imposed by the connected rigid plate of the loading frame. The axial displacement is induced at the end cross section of the bell pipe, while the end cross section of the spigot pipe remains fixed. **Figure 11** shows the deformed shape of specimen AC4-BD, and indicates a very good comparison between the experimental and numerical results.

(a)

(b)

Figure 11. Deformed shape of lap welded joint of specimen AC4-BD subjected to axial compression; (a) experiment; (b) numerical simulation.

SUMMARY AND CONCLUSIONS

The present paper reports experimental results on 24-inch nominal diameter steel pipes with welded lap joints, subjected to compressive and tensile axial loading. Two different values of thickness have been examined; 0.135 in (3.429 mm) and 0.250 in (6.35 mm), with different weld types (double, single-internal and single-external). In all specimens, the welded lap joints have been capable of sustaining remarkable axial deformation without failure. In compression experiments, no "loss of pressure containment" has been recorded despite the fact that local strains in several locations exceeded the value of 5%. In the tensile experiments, local strains that reached 8% were recorded, before fracture occurred. The significant strength and deformation capacity of these joints, under both tensile and compressive loading, indicates that lap welded steel pipe can be employed in demanding applications such as seismic areas, where severe permanent ground-induced actions are expected.

REFERENCES

Chatzopoulou, G., Fappas, D., Karamanos, S. A., Keil, B., Mielke R. D., (2018), "Numerical simulation of steel Lap welded pipe joint behavior in seismic conditions.", *ASCE Pipelines Conference*, Toronto, Canada.

Karamanos, S. A., Sarvanis, G. C., Keil, B. and Card, R. J. (2017a), "Analysis and Design of Buried Steel Water Pipelines in Seismic Areas.", *ASCE Journal of Pipeline Systems Engineering & Practice,* Vol. 8, Issue 4.

Karamanos, S. A., Koritsa, E., Keil, B. and Pappa, P. (2017b), "Mechanical Response of Steel Pipe Welded Lap Joints in Seismic Areas.", *ASCE Pipelines Conference*, Phoenix, AZ, USA.

Karamanos, S. A., Koritsa, E., Keil, B. and Card, R. J. (2015), "Analysis and behavior of steel pipe welded lap joints in geohazard areas.", *ASCE Pipelines Conference*, Paper No. 413, Baltimore, Maryland, USA.

Keil, B. D., Gobler, F., Mielke, R. D., Lucier, G., Sarvanis, G. C., and Karamanos, S. A. (2018), "Experimental Results of Steel Lap Welded Pipe Joints in Seismic Conditions", *ASCE Pipelines Conference*, Toronto, Canada.

Sarvanis, G. C, Chatzopoulou, G., Fappas, D., Karamanos, S. A., Keil, B., Mielke R. D., Lucier G., (2019), "Finite Element Analysis of Steel Lap Welded Joint Behavior under Severe Seismic Loading Conditions", *ASCE Pipelines Conference*, Nashville, Tennessee.